Alma Mater Studiorum Università di Bologna
Archivio istituzionale della ricerca

Introducing Meta-models for a More Efficient Hazard Mitigation Strategy with Rockfall Protection Barriers

(Article begins on next page)

01 May 2024

Introducing meta-models for a more efficient hazard mitigation strategy with rockfall protection barriers

David Toe · Alessio Mentani · Laura Govoni · Franck Bourrier · Guido Gottardi · Stéphane Lambert

Abstract The paper presents a new approach to assess the effecctiveness of rockfall protection barriers, accounting for the wide variety of impact conditions observed on natural sites. This approach makes use of meta-models, considering a widely used rockfall barrier type and was developed from on FE simulation results. Six input parameters relevant to the block impact conditions have been considered. Two meta-models were developed concerning the barrier capability either of stopping the block or in reducing its kinetic energy. The outcome of the parameters range on the meta-model accuracy have been also investigated. The results of the study reveal that the meta-models are effective in reproducing with accuracy the response of the barrier to any impact conditions, providing a formidable tool to support the design of these structures. Furthermore, allowing to accomodate the effects of the impact conditions on the prediction of the block-barrier interaction, the approach can be successfully used in combination with rockfall trajectory simulation tools to improve rockfall quantitative hazard assessment and optimise rockfall mitigation strategies.

D. Toe · F. Bourrier
Université Grenoble Alpes, Irstea, UR EMGR, 2 rue de la Papeterie-BP 76, F-38402 Saint-Martin-d'Hères, France
E-mail: david.toe@irstea.fr

S. Lambert
Université Grenoble Alpes, Irstea, UR ETGR, 2 rue de la Papeterie-BP 76, F-38402 Saint-Martin-d'Hères, France

A. Mentani · L. Govoni · G. Gottardi
Universita di Bologna - Via Zamboni, 33 - 40126 Bologna

1 Introduction

Rockfall hazard mitigation nowadays depends on spatial planning, protection forest management, structural measures (such as embankments, galleries or protection barriers) and monitoring. Rockfall protection barriers, i.e. flexible nets, are the most widely used structural countermeasures(Lambert and Bourrier, 2013; Calvetti and Di Prisco, 2012; Gentilini et al., 2013). Rockfall barriers are the most widely used structural countermeasures for intercepting rock blocks on their route down to the elements at risk. Barriers are typically made of different metallic components including posts, net, cables and other connecting components which makes their mechanical response very complex to predict.

As for other passive rockfall protection structures, the design of barriers, as well as the definition of the optimum protection strategy for a given site, relies on trajectory simulation results. In particular, stochastic trajectory simulation models provide statistics associated to the rock blocks paths along the slope as well as their reach probability. The design aims at reducing the latter down to a targeted value while considering the former. More precisely, relevant statistical descriptors associated to the blocks passing heights and kinetic energies are considered for determining the required protective structure characteristics in terms of interception height and kinetic energy absorption capacity respectively (Lambert et al., 2013). In practice, the barrier design for a given site is mainly based on the comparison of the statistical descriptor of the block kinetic energy with a barrier reference capacity. This capacity is often obtained following the European guideline ETAG 027 (Eota, 2013), which provides detailed indications on how to test and assess the performance of a barrier and to obtain the CE marking. Nevertheless, the impact conditions in such test, which essentially consist in an impact in the center of a 3-spans barrier by a block without any rotation, can be considered not representative of the wide variety of impact loading cases as resulting from the interception of blocks on-site. This issue has been long debated over the last ten years and several research works have suggested that a test in such conditions may not be the most critical, as it neglects the effects of parameters such as the impact point location or the incident angle of the block trajectory (Cazzani et al., 2002; Cantarelli et al., 2008; Lambert et al., 2009; Chanut et al., 2015). This suggests that current design approaches might be inadequate in accounting for the global ability of barriers in arresting the blocks, considering all the possible trajectories.

Improving the design of barriers as well as assessing their efficiency in reducing the hazard at the elements at risk requires better accounting for their actual mechanical response to blocks impacts. This may be undertaken making use of suitable numerical tool, among the various ones that have been developed over the last 20 years, with increasing complexity with either finite or discrete element models (FEM or DEM resp.) (Nicot et al., 2001; Volkwein, A., 2005; de Miranda et al., 2010; Bertrand et al., 2012; Gentilini et al., 2012, 2013; Escallòn et al., 2014; de Miranda et al., 2015; Bourrier et al., 2015;

Mentani et al., 2015; Coulibaly et al., 2017; Albaba et al., 2017). Validation by real scale experiments proved these models to be rather accurate. Nevertheless, a relatively high computational cost limits their use in view of investigating the response of barriers varying many parameters, either concerning the structure or the impact conditions.

A promising alternative of accounting for the mechanical response of barriers, for both design and hazard reduction assessment purposes, consists in using meta-models. Such approache proposes surrogate models, so called meta-models, of more complex mechanical models, embedding their complexity but are more efficient in terms of computational time (Sudret, 2008; Blatman and Sudret, 2010; Mollon et al., 2011). In the context of rockfall protection structures, the surrogate models are computationally cost-effective tools dedicated to statistical analysis of the structure response to varying impact conditions. Meta-models are widely used in civil engineering (Jin et al., 2001; Farhang-mehr and Azarm, 2005; Gonzalez-Perez and Henderson-Sellers, 2008; Toe et al., 2017). Application in the field of rockfall protection structures was first considered by Bourrier et al. (2015) with the aim of investigating the failure occurrence of a barrier via a performance function and then by Mentani et al. (2016).

This article proposes the use of meta-modelling approaches for improving the design of passive rockfall protection structures with a specific focus on a barrier intended for low kinetic energies frequently encountered in the Alpine arc. This barrier type features an interception structure made of an hexagonal wire mesh supported by longitudinal cables passing through steel posts. A finite element (FE), three-dimensional, non-linear model of the barrier has been developed and subjected to impact simulations by varying simultaneously 6 impact parameters over a wide and a comparatively narrower range. The results of the analyses provides a thorough insight of the protection barrier behaviour in terms of failure mechanisms and enables to explore comprehensively its effect on the energy possessed by the impacting block. Meta-models of the barrier response in terms of block arrest and block kinetic energy reduction have been developed, considering two sets of impact condition parameters. The first set has been defined based on the widest possible range for each parameter. The second set has been adapted to the barrier capacity evaluated in standard conditions.

The article is organised as follows. In the first section, details of the FE models and FE analyses are given and results are discussed in terms of block-structure interaction, revealing the complexity of the barrier response to impact. In the second section, the development of meta-models of the barrier response is detailed. Then, the meta-model results are presented and discussed in terms of accuracy. The discussion addresses the influence of the parameter ranges on the meta-models accuracy, the benefits in using these meta-models compared to current design approaches, and their application to real cases.

2 Finite element modelling of a cable-net barrier

This section provides the details of the finite element (FE) modelling of a cable-net barrier, developed using the commercial code Abaqus (Abaqus, 2013). For this barrier type, the interception structure is made of longitudinal cables, connected to steel posts fully restrained at the base. In general, this structure type is also provided with a secondary hexagonal meshwork fastened to the longitudinal cables. Although widely used, information on the response to impact of this barrier type are scarce. The results of the FE analyses then offer a new insight on the barrier mechanical behaviour, while providing the necessary base to the development of a meta-model of the block-barrier interaction.
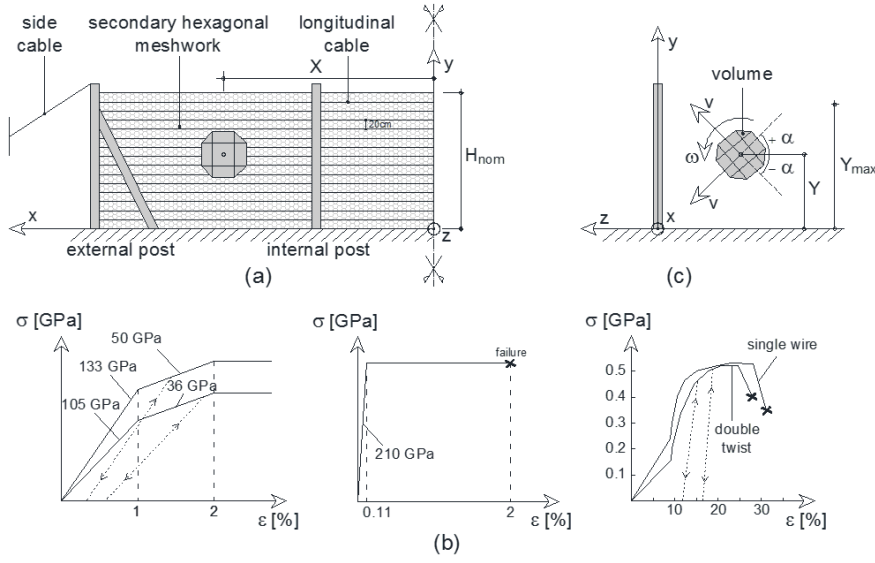
Fig. 1 Geometry and impact conditions for the cable-net protection barrier: a) back view, b) stress-strain behaviour of cables, posts and net and c) side view.

2.1 FE model

As described in Fig. 1a, the study considers a three spans, 5 m spaced, cable-net barrier of 3.2 m nominal height. Longitudinal cables, 12 mm in diameter, pass through the internal posts (IPE 200) and are knotted to the external posts (IPE 300), connected to the ground by side cables of 18 mm diameter. A secondary meshwork, made of a double twisted hexagonal mesh is connected to the top and bottom longitudinal cables with steel wires. The FE model of the barrier is three-dimensional and made of one-dimensional elements, whose

behaviour is governed by elasto-plastic constitutive laws. The mechanical response of the barrier elements was described based on available results of laboratory tests in de Miranda et al. (2015). The contacts between block and barrier and between the barrier elements (cables and net) were modeled with a Coulomb-type frictional behaviour with a coefficient of 0.4 (de Miranda et al., 2015). Particular attention was devoted to model the behaviour of the wires within the hexagonal mesh, following data of experiments carried out on mesh portions (Mentani et al., 2015; Thoeni et al., 2013). A representative scheme of the stress-strain curve for each structural element is given in Fig. 1b, where the relevant model parameters are also inserted. As depicted, the posts behave following an elastic-perfectly-plastic law up to a failure limit, cables harden in the plastic phase and may undergo indefinite deformations once a second yielding threshold is attained and mesh wires soften prior to fail.

2.2 FE simulations and results

The barrier model was subjected to non-linear dynamic simulations. According to the reference system and notation introduced in Fig. 1, simulation were carried out, by impacting the barrier model with a prismatic test block of known volume V; at a position of coordinates X and Y; with an incident angle α; a translational velocity v; and a rotational velocity ω.

The first simulations were performed in accordance to the procedure described in the Annex A of ETAG 027 (Eota, 2013), to provide the cable-net barrier model with a reference capacity evaluated in standard conditions. In these simulations, a translational velocity of 25 m/s and no rotational velocity were considered. The maximum block mass for which all the guideline requirement were fullfilled, was found equal to 640 kg, yielding a reference capacity of 200 kJ for the cable net barrier. It is worth highlighting that this latter value is not the ultimate kinetic energy the barrier is able to withstand, as it was obtained increasing the mass by steps so that the kinetic increase from one case to the following was 25 kJ. The 225 kJ impact led to rupture but not the 200 kJ one.

Further analyses were then run to provide the data necessary to the development of meta-models of the barrier response. To this purpose, parameters related to the block were varied. Table 1 collects these parameters along with their variation ranges, according to the notation introduced in Fig. 1. As indicated in this table, two sets of parameters with different ranges were considered in this study for generating virtual test programmes: a wide range set (WR) and a narrow range set (NR) .

The wide range (WR) set was considered in agreement with possible output of rockfall trajectory simulations and results of field tests (Bourrier et al., 2009a; Toe et al., 2017). As it is observed in Table 1, a freeboard on the barrier top was inserted, to avoid direct impacts of blocks on the top cable. A total of 280 simulations were carried out using combinations of the input parameters.

Table 1 Input parameters for loading conditions.

Input parameter	unit	Wide Range (WR) min-max	Narrow Range (NR) min-max
Translational velocity, v	m/s	5 - 40	5 - 22.5
Rotational velocity, ω	rad/s	0 - 35	0 - 35
Volume of the block, V	m^3	0.03 - 4	0.03 - 2.5
Incident angle, α	deg	-60 - 60	-60 - 60
Impact position, X	m	0 - 7.5	0 - 7.5
Impact position, Y	m	1 - 2.5	1 - 2.5

The programme of tests resulted from a Latin-Hypercube sampling, assuming a uniform distribution of values within the parameter ranges (Sacks et al., 1989; Fang et al., 2005).

(a) Block rolling over the barrier: v = 11.7 m/s; ϖ = 7.15 rad/s; V = 2.26 m³; X = 1.08 m; Y = 1.57 m; α = -46.5°

(b) Block puncturing the secondary mesh: v = 5.97 m/s; ϖ = 16.6 rad/s; V = 0.59 m³; X = 3.56 m; Y = 1.49 m; α = 24.8°

(c) Block producing global failure of the barrier: v = 27.99 m/s; ϖ = 20.3 rad/s; V = 3.21 m³; X = 5.67 m; Y = 1.84 m; α = -1.86°
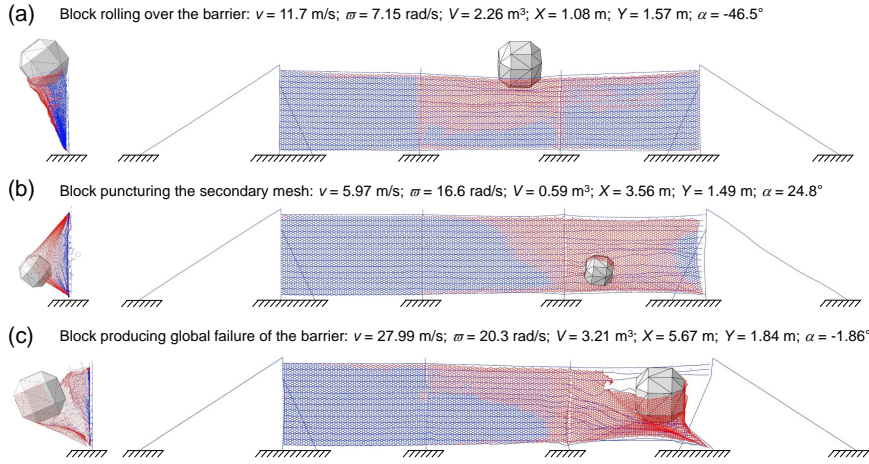
Fig. 2 Block-barrier interaction mechanisms: a) block rolling over; b) mesh perforation and c) global failure.

The results of this set of simulations provided new evidence of the barrier response considering a wide variety of realistic loading conditions. In particular, four types of block-barrier interactions were observed, which can be described as follows: i) the block is arrested by the barrier; ii) the block passes the barrier by rolling over it; iii) the block passes the barrier as a result of the perforation of the secondary hexagonal meshwork; iv) the block passed the barrier as a result of the failure of the whole structure.
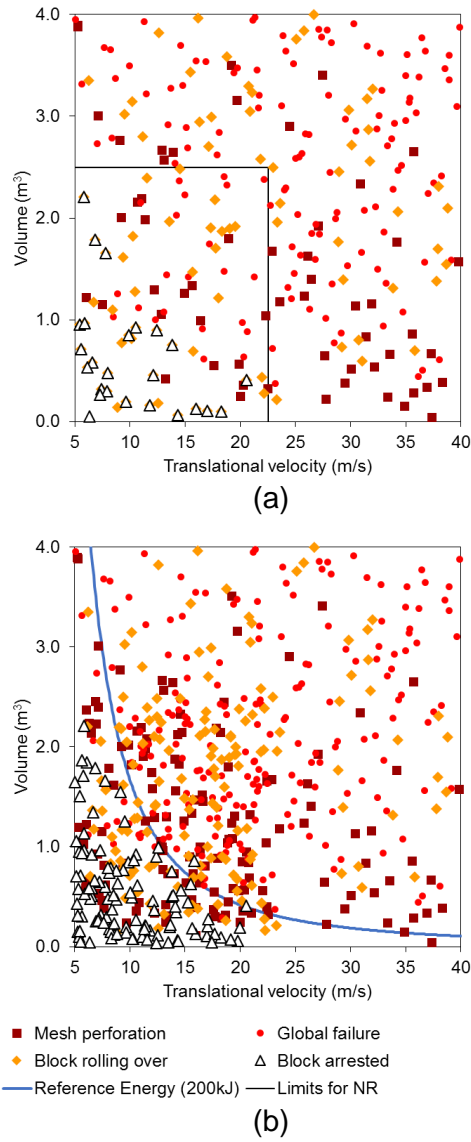
Fig. 3 Results of the analyses on the translational velocity - volume plane: a) wide range and b) wide range and narrow range.

Fig. 2 illustrates the front and side views of the deformed barrier through the last instants of three selected impact simulations, where the elements which have entered the plastic domain are coloured in red. In all these FE tests, the barrier resulted unable to stop the impacting block. In particular, Fig. 2a provides an example of the rolling over mechanism, with the block overcoming the barrier, Fig. 2b depicts the barrier failing due to the perforation of the

hexagonal net at a side span. Finally, global failure of the barrier is shown in Fig. 2c, with clearly visible formation of plastic hinges at one external post, detachment of longitudinal cables and ruptures within the secondary meshwork.

In Fig. 3a, the results of the simulations are grouped on the block translational velocity - block volume plane, using symbols according to the observed block-barrier interaction mechanism. Over the 280 simulations, the barrier succeeded in stopping the block in 26 cases. In 254 cases the barrier failed to stop the block: in 65 cases due to the block rolling over mechanism, in 57 cases due to mesh perforation and in 132 cases due to global failure. This low barrier success ratio is associated to the large ranges considered, without any restriction related to the capacities of the barrier. In fact, the points relevant to arrested blocks are characterized by velocities lower than 22.5 m/s and by block volumes smaller than 2.5 m^3.

A further set of 280 simulations was then performed to obtain more information on the barrier response within these threshold values, and thus supplying more data for the development of a meta-model of the barrier ability to arrest a block. In these new FE tests, the translational velocity and volume were varied within this comparatively narrower range, according to the limit value indicated in Table 1. As for the wide range, the virtual test programme was designed based on the Latin-Hypercube sampling procedure.
Over the 280 simulations, the barrier succeeded to stop the block in 61 cases. In 219 cases the barrier failed to stop the block : in 78 cases due to the block rolling over mechanism, in 66 cases due to mesh perforation and in 75 cases due to global failure.

Fig. 3b gather the 560 simulation results from the analyses conducted considering the narrow and wide range sets. The locus of kinetic energy equal to the determined reference capacity (iso-energy line at 200 kJ), is also inserted in Fig. 3b. The vast majority of the points corresponding to the arrested blocks falls below this line. However, cases of barrier failures in arresting the block are also found below this line. In total, the ratio of observed failure cases to the total number of cases below this line is as high as 52%. This comment holds for moderate block volumes and velocities. Indeed, restricting the analysis to cases where the block size is less than 1/3 the barrier height (thus to block volumes less than 0.7 m^3 and as suggested by ETAG 027 (Eota, 2013)), this ratio equals 33.7%. This suggests that the use of a unique reference capacity value might be unconservative for this barrier.

2.3 Effects of the impact parameters on the barrier response

Fig. 4 illustrates the influence of the other impact parameters on the barrier response: the incident angle (Fig. 4a), the rotational velocity (Fig. 4b), the impact position (Fig. 4c - 4d). For negative values of incident angle (upward tra-
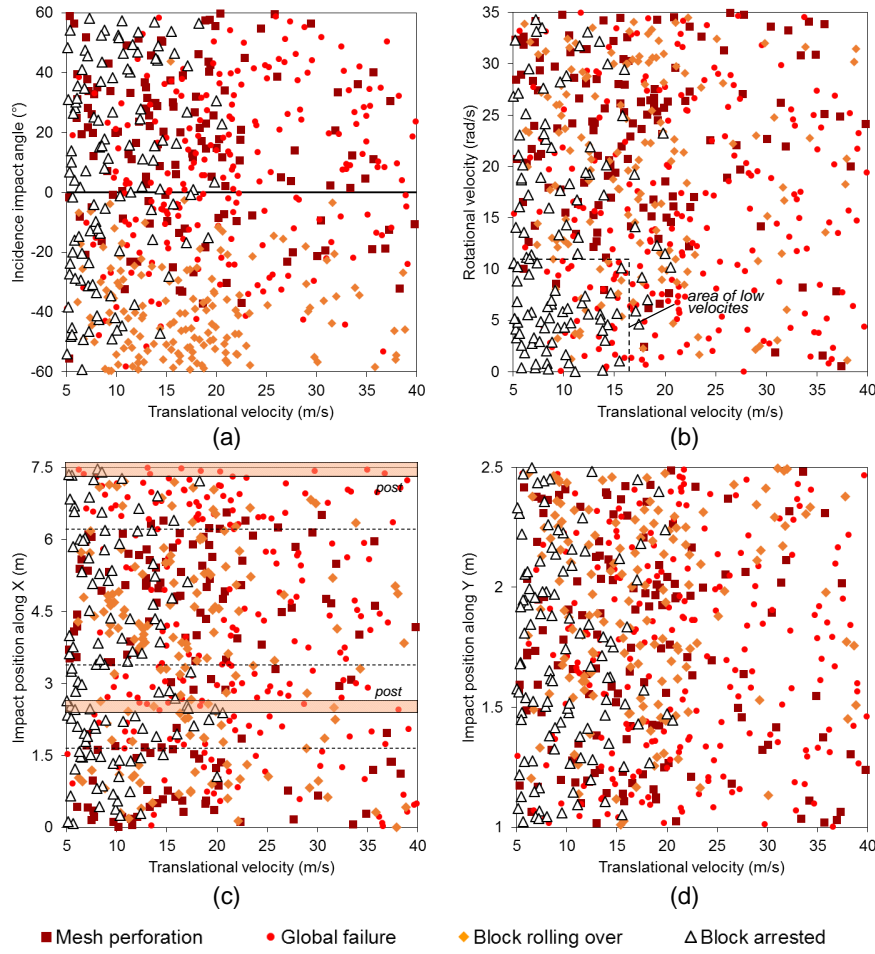
Fig. 4 Results of the analyses as a function of: a) incident impact angle, b) rotational velocity, c) and d) impact position.

jectory), the rolling over mechanism is the prevailing block-barrier interaction mode (Fig. 4a). On the velocity plane, although symbols related to arrested blocks tend to concentrate in the area close to the origin, several points also prove the ability of the barrier to stop impacting blocks with high rotational velocities, up to 35 rad/sec (Fig. 4b). As shown in Fig. 4c, the points relevant to the general failure mechanism tend to concentrate close to the posts, whose location is highlighted with two hatched areas along the y-axis (position X in Fig. 1). This is particularly clear for translational velocities less than 20 m/s and general failures are observed at velocities down to 5 m/s.

The influence of the impact position of the block along the y-axis is depicted in Fig. 4d. As it is observed, high values of block velocity and position tend to

result in a rolling over mechanism, whereas no significant effects of the position parameter is observed on the barrier ablity of arresting the block, which remains prevalently driven by the block speed. This is also due to the considered freeboard introducing a threshold in the impact height with respect to the barrier height.

In Fig. 5, the results of the simulations are plotted on the volume-kinetic energy plane up to 600 kJ and compared with the reference energy line. In Fig. 5a the kinetic energy is computed by considering the sole contribution of the translational component, while in Fig. 5b the total kinetic energy is used, accounting for both the translational and the rotational kinetic energies. Comparison shows that, although the upward shifting of the data points from Fig. 5a to Fig. 5b produces a migration of some arrested block points above the reference energy line (equaling 200 kJ), there are still several cases below the line, in which the barrier failed in arresting the block, due to mesh perforation, global failure and block rolling over mechanisms.
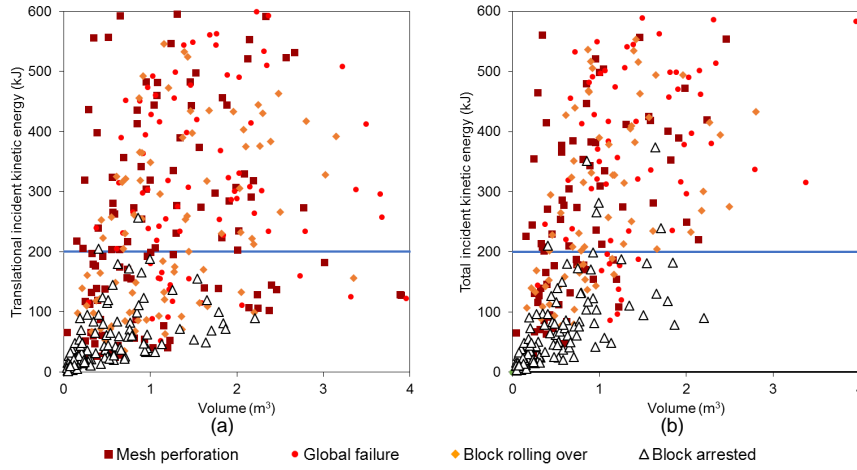
Fig. 5 Results of the analyses as a function of: a) incident impact angle, b) rotational velocity, c) and d) impact position.

Overall, the results show a strong dependency of the barrier response to the impact conditions. Analysis of the data also showed that, although some trends could be observed, a clear correlation between input parameters and relevant block-barrier interaction mechanisms could not be established with certainty. These results bring to light the shortcomings of deterministic approaches based on a single impact assessment test, towards the evaluation of a structure effectiveness, as not adequately accounting for the impact conditions. This crucial aspect can be more successfully accommodated by reliability probabilistic approaches, through the use of meta-models which allow for the

prediction of the barrier response as a function of the impact conditions, as described in the following sections.

3 The meta-modeling approach

This section provides the essential details of the meta-modelling strategy used in this study.

Meta-models can be defined in this context as mathematical operators describing the response envelop of a given structure, by considering a large number of variables. With reference to a rockfall protection structure, a meta-model can be developed from an optimized number of numerical simulations, performed using a detailed numerical model of the protection work, allowing for the prediction of its response to any set of variables, without running extra simulations. Due to its mathematical structure and computational cost-effectiveness, a meta-model can be integrated into probabilistic rockfall trajectory models rather easily.

Within the context of rockfall hazard assessment, it is important for a meta-model to capture with accuracy the effects of the structure on the falling block in terms of trajectory and post-impact kinetic energy. In the light of these general observations, this study focuses on two essential and correlated aspects of the block-barrier interaction, which are the barrier ability to arrest a block and, in case of failure, the block post-impact kinetic energy. To the scope, two different meta-models were developed for these two aspects using classical meta-modeling techniques.

Two meta-models were developed using the results of the FE simulations carried out on the cable-net barrier. Each meta-model was developed considering six input parameters (V, v, ω, α, X and Y) varying for two ranges (WR and NR - Table 1). The first meta-model is created to predict the success (B_{Succ}) or failure (B_{Fail}) of the barrier in arresting the block. As dealing with two classes, a Support Vector Machine (SVM), was used for creating the meta-model (Brereton and Lloyd, 2010; Kausar et al., 2011). The second meta-model was developed to predict the block kinetic energy reduction due to the block-barrier interaction for the B_{Fail} cases. The value of energy reduction is given as the difference between the total (translational plus rotational) kinetic energy posses by the block just prior to the impact and the total kinetic energy possessed by the block just after the impact ($E_{incident} - E_{out} = E_{RED}$). The total kinetic energy was considered in order to account for possible coupling between translational and rotational velocities, after and before impact. The Kriging method has been used (Kleijnen, 2009; Martin, 2009) to build this second meta-model. Main features of these two meta-modeling approaches are given in the following sections.

3.1 Support Vector Machine

The Support Vector Machine (SVM) approach is based on statistical learning theory (Vapnik, 1995), and can be used to build a meta-model which can predict the class of an output data. This method has been used in many different fields of study as for examples remote sensing (Mountrakis et al., 2011), shape recognition (Ma and Ding, 2002), genomics recognition (Sonnenburg et al., 2005) and spam detection (Maldonado and LHuillier, 2013). This method is adapted for binary or multi-class recognition and is here used for the former (success/failure of the barrier).

The basic SVM approach (M_{SVM}) consists of defining, in a space of input parameters, the optimal hyper-plane separating the regions associated with the different classes (success/failure of the barrier in this context). For that purpose, among all points of the space only those that are closest to the hyperplane, called support vector, are considered. The optimal hyperplane is defined as the hyperplane whose margin, i.e. distance from these closest points is maximal. It is thus calculated by maximizing the distance from the hyperplane to the closest points on each side.

The optimal definition of the hyperplane can require non linear transformation of the data to another space of potentially higher dimension using kernel functions (Baudat and Anouar, 2001).

In this study, the space of the input parameters corresponds to the different parameters associated with the impact conditions. Linear and radial kernels have been used to build accurate meta-models (function *svm* in R (V 3.2.3) package *e1071*). The meta-model created is defined as a R function which can be coupled with a rockfall trajectory analysis tool to predict success or failure of the barrier.

3.2 Kriging

The Kriging (Gaussian process modeling) approach is a procedure of interpolation which is used in various engineering and applied mathematical problems (Simpson et al., 2001; Sudret, 2012; Zhang et al., 2014). This method is well adapted for approximating results of deterministic models, such as the post-impact kinetic energy of the block in this study (Martin, 2009). Kriging models are generally described as the combination of a deterministic component, defined by a regression model, with a stationary Gaussian process associated with a constant variance and a correlation function. Contrary to polynomial regression models, Kriging models do not only assume an underlying global functional form. They can approximate arbitrary functions with high global and local accuracies.

In this study, the meta-model based on a Kriging approach (M_K) is developed using the matlab tool box *UQLab* (Marelli and Sudret, 2014) which enables the creation of an efficient Kriging predictor based on small number of data. A 3rd order polynomial regression model was used for the deterministic

component of the Kriging model. Following recommendations for a default use in *UQLab* (Marelli and Sudret, 2014), an ellipsoidal Matern function was set as correlation function. The second meta-model created is defined as a matlab function which can be coupled with a rockfall trajectory analysis tool to predict the kinematic energy lost by the block after impact on the barrier.

3.3 Error quantification

The accuracy of the developed meta-models was estimated by comparison with the data obtained from the FE simulations described and illustrated in Section 2. The prediction error for both meta-models was estimated using the leave-one-out cross validation method (Allen, 1971).

For the SVM approach based meta-model, n results $M(x_i)$ from the FEM simulations are considered. For each parameters combination x_i, a meta-model is created using all FEM simulation results except $M(x_i)$. The meta-model prediction for x_i ($M_{SVM}^i(x_i)$) is compared to the remaining result $M(x_i)$ observed from the FEM simulations. This comparison is repeated for all x_i ranging between x_1 and x_n. The global accuracy of the meta-model ($Q(M_{SVM})$) is evaluated as follows :

$$Q(M_{SVM}) = 1 - \frac{1}{n}(\sum_{i=1}^{n} M(x_i) - M_{SVM}^i(x_i)) \tag{1}$$

The results of the SVM based meta-model were further discussed with reference to the misclassification rate defined as follows. With reference to the FE observations, the SVM based meta-model can provide bad (false, F) or good prediction (true, T). As described in Table 2, a false prediction can be positive (FP) if a barrier success (B_{Succ}) is estimated for a case in which failure (B_{Fail}) was observed; a false prediction can be negative (FN) if a barrier failure (B_{Fail}) is estimated for a case in which a success (B_{Succ}) was observed. In a similar way, good prediction can be positive when the barrier success (B_{Succ}) is both estimated and observed and negative when the barrier failure (B_{Fail}) is both estimated and observed. Based on these definitions, two indicators were used to discuss the performance of the SVM based meta-model: the false negative rate ($FN_r = \frac{FN}{FN+TP}$) and the false positive rate ($FP_r = \frac{FP}{FP+TN}$). In the context of this study, the false positive rate ($FP_r = \frac{FP}{FP+TN}$) is the most relevant to deal with as it focuses on the most critical situation. In fact, a high FP_r value is associated to an overestimation of the barrier capacity by the meta-model, with the meta-model erring on the unconservative side.

For the Kriging approach based meta-model, a similar leave-one-out cross validation method as for the SVM approach based meta-model was used. The values of the residual block kinetic energy predicted by the meta-model $M_{E,K}^i(x_i)$ were compared to those obtained from the FE simulations ($M_E(x_i)$). The accuracy of the meta-model is evaluated using the mean ($Mean_{Err}$) and

Table 2 Definition of cases for assessing the meta-models performance

	SVM prediction	
FE observation	B_{Fail}	B_{Succ}
B_{Fail}	TN	FP
B_{Succ}	FN	TP

standard deviation (Sd_{Err}) of the residual error. $Mean_{Err}$ was calculated as:

$$Mean_{Err} = \frac{1}{n} \sum_{i=1}^{n} (M_E(x_i) - M_{E,K}^i(x_i)) \tag{2}$$

Sd_{Err} is calculated as:

$$Sd_{Err} = \sqrt{\frac{\sum_{i=1}^{n} (M_E(x_i) - M_{E,K}^i(x_i))^2}{n} - Mean_{Err}^2} \tag{3}$$

4 Meta-models of the cable-net barrier

In this section the results of the meta-models of the cable-net barrier described in Section 2 are illustrated and discussed. The validation of the meta-models was pursued by comparison with the data obtained by the FE simulations. Focus is placed on the influence of the parameters range on the performance of the considered meta-models.

4.1 Wide range based meta-models

This section presents and discusses the results from the two meta-models developed based on the wide range set FE simulations (WR, Table 1).

Results of the meta-model addressing the ability of the barrier in stopping the block are given in Fig. 6 where symbols in grey stand for good prediction by the meta-model compared to FE simulations results. Bad predictions are grouped as positive (red) or negative (yellow) according to the definition given in Table 2. In particular, as described in Table 3, the meta-model failed to predict 8 out of 26 barrier success ($FN_r = 32\%$) and 5 out of 254 barrier failure ($FP_r = 2\%$). Over the 5 misclassified failures of type FP, 1 was related to mesh perforation, 3 were related to global failure and 1 was related to block rolling over the barrier. It can be concluded that the barrier efficiency in arresting the block is slightly overestimated as only 2% of the failure cases are not predicted by the meta-model. The global accuracy of the meta-model, $Q(M_{SVM})$, was found equal to 95% according to eq. 1.

The meta-model dealing with the block kinetic energy reduction was created excluding the 26 simulations in which the block were stopped by the barrier. According to eq. 2 and 3, the mean error, $Mean_{Err}$, and standard

Table 3 SVM based meta-model: wide range results

	Prediction		
Observation	B_{Fail}	B_{Succ}	
B_{Fail}	249	5	$FP_r = 2\%$
B_{Succ}	9	17	$FN_r = 35\%$
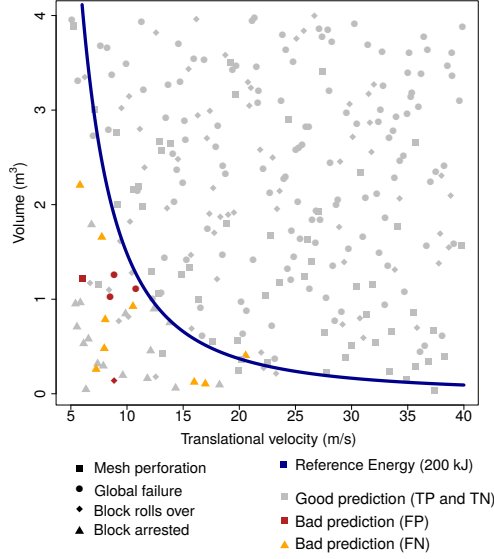
Fig. 6 Prediction of B_{Succ} and B_{Fail} as a function of the block volume and translational velocity for the wide range scenario.

deviation, Sd_{Err} of the M_K, are 0.52 kJ and 200 kJ respectively. The former value indicates that the meta-model prediction is unbiased, with the practical implication that there are as many unconservative predictions than conservative ones. The latter value appears rather high compared to the barrier reference capacity.

The black curve on Fig. 7 gives the cumulative distribution of the difference between the energy reduction observed in the FE simulations ($M(x_i)$) and the corresponding value as predicted by the meta-model ($M_k(x_i)$) normalised by the incident block kinetic energy (E_{in}). Cases where the block kinetic reduction predicted by the meta-model is higher than values observed in the FE simulations correspond to negative ratio values, and reveal an error on the unconservative side. On the contrary, error on the conservative side consists in cases where the predicted energy reduction is less than the observed value, corresponding to positive ratio values. In 5% of the cases, the overestimation of the barrier capacity in reducing the block kinetic energy prediction by the meta-model exceeds 50 % of the incident block kinetic energy.
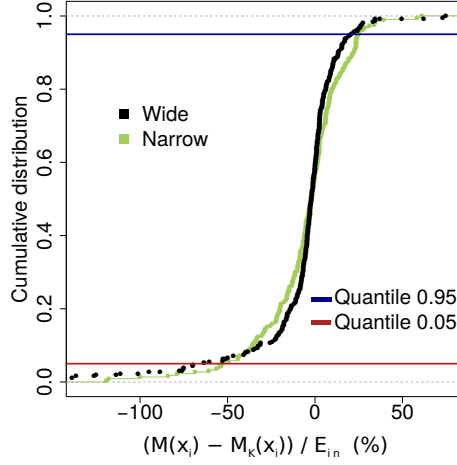
Fig. 7 Cumulative distribution of the ratio between the prediction error $(M(x_i) - M_K(x_i))$ of the block energy reduction after the impact on the barrier and the total incident block kinetic energy E_{in} for the wide (black) and narrow (green) ranges sets.

4.2 Narrow range based meta-models

The meta-models for the narrow range analysis were created using the second plan of experiments consisting of 280 combinations of the 6 input parameters (NR, Table 1).

The accuracy of the model dealing with the barrier block arresting ability was evaluated according to eq. 1 and resulted in M_{SVM} equal to 92%. The meta-model failed to predict 16 barrier success over 61 ($FN_r = 27\%$) and failed to predict 6 barrier failures over 219 ($FP_r = 3\%$) (Table 4). Over these 6 misclassified cases, 5 are related to mesh perforation and 1 is related to global failure (Fig. 8).
Here again, the meta-model overestimates the barrier capacities and 3% of the failure cases are not predicted by the meta-model.

Table 4 Quality evaluation for the meta-model created for narrow range values.

Observation	Prediction		
	B_{Fail}	B_{Succ}	
B_{Fail}	213	6	$FP_r = 3\%$
B_{Succ}	16	45	$FN_r = 27\%$

As for the meta-model concerning the block kinetic energy reduction, the mean error, $Mean_{Err}$, and standard deviation, Sd_{Err}, of the M_K are -5.21 kJ and 111 kJ respectively. The same comments as for the wide range results hold.
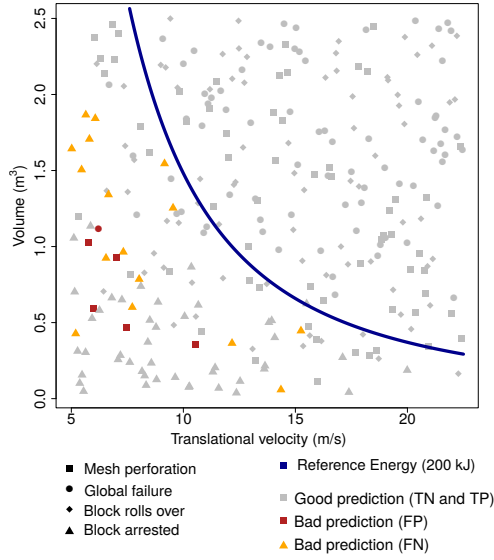
Fig. 8 Prediction of the of B_{Succ} and B_{Fail} for the narrow range scenario. Good and bad predictions are indicated by grey and red symbols receptively. The shape of the symbols indicate the mode of failure.

Neverthless, the lower standard deviation indicates that the NR meta-model is more efficient in predicting the block kinetic energy reduction.

5 Discussion

This section first discusses the influence of the range considered based on the results from the two approaches (WR and NR). It then addresses the advantages of a meta-model-based design over classical design approaches, before introducing aspects to be improved.

5.1 Influence of the range considered

The meta-models have been developed considering two ranges of values for the input parameters. Intuitively, a meta-model developed for a range of input parameters fitted to the barrier reference capacity is expected to provide much better results.

Similar trends in terms of model quality are observed for both meta-models and the difference between meta-models developed for narrow and large ranges is not that pronounced. As for the M_{SVM} almost the same global accuracy is obtained for wide and narrow ranges (92/95.3%). A significantly smaller FP_r rate is observed for the narrow range (27/32 %). In addition, the model developed for the narrow range accounts for a larger number of arrested blocks

over the 300 simulations. Its ability in detecting success cases is thought to be higher.

As for the the prediction of the block kinetic energy reduction, both models have a $Mean_{Err}$ around 0 kJ. However, the predictions M_K are significantly more accurate for the narrow range compared to that for the wide range. Indeed, the error standard deviation of the meta-model based on the narrow range is almost half that of the meta-model based on the wide range (111 kJ compared to 200 kJ).

In the end, the difference between the two meta-models appear rather small, the narrow range resulting in a slightly more accurate meta-model. Results obtained using the narrow range are considered in the following section.

5.2 Benefits of the meta-models

The current design practices are mainly based on the barrier reference capacity. In this study, the reference barrier capacity was considered as the value obtained from impacts following the recommendations of the European guideline ETAG 027 (Eota, 2013). A straightforward design for this specific barrier would consider that all the block having a kinetic energy less than 200 kJ are stopped. Similarly, the block kinetic energy reduction by this barrier would be computed as the block incident kinetic energy minus 200 kJ.

As for the efficiency of the barrier in arresting the block, results presented in section 2 have shown the limits of an assessment based on the barrier reference capacity, while section 4 has suggested the interest of meta-models. A detailed analysis of the results presented in Fig. 8 shows that the prediction by the meta-models below the reference energy line results in 4.8% of False Positive cases while considering the barrier reference capacity as a criterion led to a value of 52% (see Fig. 3). Restricting the comparison to a block size of 0.7m leads to values of 4.54% for the meta-model compared to 33.7 % for the barrier reference capacity based approach. This means that the latter is far too optimistic with respect to the ability of the barrier in stopping the blocks and that the latter is more realistic, demonstrating the benefit in using this meta-model for design or hazard assessment purpose.

As for the kinetic energy reduction, Fig. 9 compares estimates based on the barrier reference capacity and that from the meta-model. The former is obtained substracting 200 kJ to the block total incident kinetic energy. The full curve is not shown as for large kinetic energies no difference is observed from one curve to the other. Negative block output kinetic energies result from the fact that in some cases the block incident kinetic energy is less than the barrier reference capacity. These cases are accounted for in Fig. 9 but should be neutralised setting the kinetic energy to zero. The same comment holds for results from the meta-model. Fig. 9 shows that the meta-model M_K fits rather well with the simulation results (in green). On the contrary, results based on the barrier reference capacity shows important difference with the

simulation results, between 0 and 150 kJ. In fact, the kinetic energy reduction is overestimated when using the barrier reference capacity. The overestimation by the meta-model is much less and is limited to the 0-50kJ range. Beyond 200 kJ, the two approaches are similar.
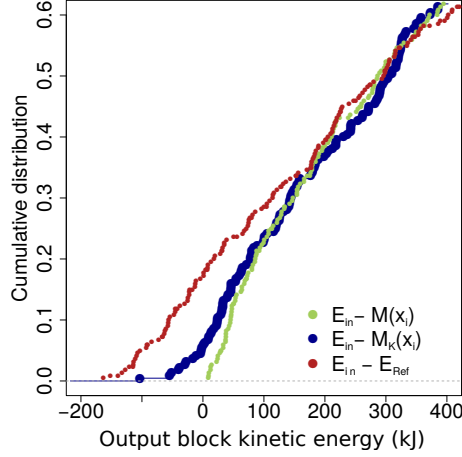

Fig. 9 Comparison between the cumulative distribution of the output kinetic energy predicted by the FE model ($E_{in}-M(x_i)$ in green), the narrow range meta-model ($E_{in}-M_K(x_i)$ in blue) and the reference capacity of the barrier ($E_{in} - E_{Ref}$ in red).

5.3 Towards application to real sites

In the previous section, the benefit in using meta-models has been demonstrated, in particular by comparison with approaches based on the direct use of the barrier reference capacity. The study has shown, that, at least, for the barrier considered, meta-models are much more efficient in assessing the barrier response.

It is worth highlighting that the considered impact conditions did not consider biased trajectories nor rotational velocities around all block axes. This simplification is thought not to call into question the conclusions drawn and is assumed to be of negligible influence on the developed meta-models accuracy.

The meta-models were developed considering all the possible impact conditions, and thus are able to mimic the barrier response whatever the impact case. However, the different impact scenario within the given parameters ranges were considered equiprobable, which is not realistic. The impact conditions depend on the block trajectories as observed on real sites. This means that the statistics in relation to the barrier response that are presented in the previous section, including the comparison with the barrier reference capacity,

should not be considered for a real site. In lieu the statistics associated to the ability of the barrier in arresting the blocks for a given site should be based on the distribution of trajectories of that site. As a consequence, the next steps will consist in assessing the efficiency of this barrier for a real site. In this aim, the next development will consist in implementing the meta-models in rockfall trajectory simulation code for a fast and accurate assessment of the barrier effect on the blocks trajectory.

The second meta-model was developed with the aim of evaluating the reduction in kinetic energy of the block, in case of barrier rupture. Such an event would also result in a change of the block propagation direction. Implementation of the kinetic energy reduction meta-model in a rockfall trajectory simulation tool would require making assumptions on the block trajectory changes after impact. Significant improvement would consist in a meta-model of the block velocity changes, but tackling the problem of building such a meta-model is a very difficult task because it entails input and output random variables that are statistically dependent. It is a very difficult problem that was already tackled in 2D for rebound (Bourrier et al., 2009b).

6 Conclusion and perspectives

In this article the application of meta-modelling techniques to rockfall protection structures, focusing on a specific barrier intended for low block kinetic energies has been proposed.

The results of 560 FE simulations showed that the barrier efficiency in arresting the block depends not only on the block volume and its translational velocity but it is also controlled by other parameters related to the block trajectory. As a consequence, quantifying the barrier efficiency without accounting for their influence may lead to unconservative estimates. For instance, 33.7 % of the impact cases below the reference barrier capacity, as deduced from a normal-to-the-fence and centered impact, in fact leads to barrier failure in arresting the block.

Two meta-models have been developed, based on the results of the 560 FE simulations: one concerning the ability of the barrier to arrest the block, the other concerning its ability in reducing the block kinetic energy in case of barrier failure in arresting the block. Two parameters ranges were considered for creating these two meta-models. The one closer to the barrier reference capacity appears to be slightly more accurate. Nevertheless, the difference being small, no optimisation is required with respect to the definition of the ranges for creating a reliable meta-model. Overall, the meta-models have been shown to provide an accurate prediction of the barrier response. In particular, the meta-model unconservative error associated to the ability of the barrier in arresting the block is less than 5%, compared to 33.7 % following a straightforward design approach. This clearly demonstrates that meta-models represent a promising approach for improving the design of protective structures, and consequently the rockfall risk mitigation.

One possible limitation in the followed methodology is the number of barrier response simulations required for creating a meta-model. In this case, 280 FE simulations were used while considering 6 variable input parameters. This could be a problem while dealing with a larger number of variables or using more computationally demanding barrier numerical models. One perspective to this work would be to reduce the necesssary numerical simulations without altering the meta-model accuracy.

The meta-models have been developed with the final aim of quantifying the real efficiency of the barrier in reducing the hazard or the block kinetic energy downhill. The next step will consist in introducing the meta-models in rockfall trajectory simulations. This will allow accounting for the real distributions of the various parameters describing the possible block trajectories and will represent a significant improvment in quantitative rockfall hazard assessment in presence of a protective barrier (Corominas et al., 2005).

Meta-models may also be used for helping in the optimisation of the design of rockfall barriers, allowing for the identification of detrimental mechanisms leading to structure failure. In this case, parameters related to the design of the structures may be considered, such as the position and initial tension of the cables, post spacing, position of energy dissipating device, if present. This does represent an inspiring perspective for manufacturers, designers and researchers.

References

Abaqus (2013). Abaqus Analysis Users Manual. Version 6.11.

Albaba, A., Lambert, S., Kneib, F., Chareyre, B., and Nicot, F. (2017). DEM modeling of a flexible barrier impacted by a dry granular flow. *Rock Mechanics and Rock Engineering (Accepted)*.

Allen, D. M. (1971). *The Prediction Sum of Squares as a Criterion for Selecting Predictor Variables*. University of Kentucky.

Baudat, G. and Anouar, F. (2001). Kernel-based methods and function approximation. In *Proceedings of International Joint Conference on neural networks*, volume 2, pages 1244–1249.

Bertrand, D., Trad, A., Limam, A., and Silvani, C. (2012). Full-Scale Dynamic Analysis of an Innovative Rockfall Fence Under Impact Using the Discrete Element Method: from the Local Scale to the Structure Scale. *Rock Mechanics and Rock Engineering*, 45(5):885–900.

Blatman, G. and Sudret, B. (2010). Efficient computation of global sensitivity indices using sparse polynomial chaos expansions. *Reliability Engineering & System Safety*, 95(11):1216–1229.

Bourrier, F., Baroth, J., and Lambert, S. (2015). Accounting for the variability of rock detachment conditions in designing rockfall protection structures. *Natural Hazards*, 81(1):365–385.

Bourrier, F., Dorren, L., Nicot, F., Berger, F., and Darve, F. (2009a). Toward objective rockfall trajectory simulation using a stochastic impact model. *Geomorphology*, 110(3):68–79.

Bourrier, F., Eckert, N., Nicot, F., and Darve, F. (2009b). Bayesian stochastic modeling of a spherical rock bouncing on a coarse soil. *Nat. Hazards Earth Syst. Sci.*, 9(3):831–846.

Brereton, R. G. and Lloyd, G. R. (2010). Support Vector Machines for classification and regression. *Analyst*, 135(2):230–267.

Calvetti, F. and Di Prisco, C. (2012). Rockfall impacts on sheltering tunnels: real-scale experiments. *Geotechnique*, 62(10):865–876. WOS:000308697900001.

Cantarelli, G., Giani, G., Gottardi, G., and Govoni, L. (2008). Modelling rockfall protection fences. In *Proceedings of the 1st World Landslide Forum*, pages 103–108, Tokyo, Japan.

Cazzani, A., Mongiov, L., and Frenez, T. (2002). Dynamic finite element analysis of interceptive devices for falling rocks. *International Journal of Rock Mechanics and Mining Sciences*, 39(3):303–321.

Chanut, M.-A., Dubois, L., and Nicot, F. (2015). Dynamic Behavior of Rock Fall Protection Net Fences: A Parametric Study. In *Engineering Geology for Society and Territory - Volume 2*, pages 1863–1867. Springer, Cham. DOI: 10.1007/978-3-319-09057-3_330.

Corominas, J., Copons, R., Moya, J., Vilaplana, J. M., Altimir, J., and Amig, J. (2005). Quantitative assessment of the residual risk in a rockfall protected area. *Landslides*, 2(4):343–357.

Coulibaly, J. B., Chanut, M., Lambert, S., and Nicot, F. (2017). Nonlinear Discrete Mechanical Model of Steel Rings. *Journal of Engineering Mechanics*, 143(9).

de Miranda, S., Gentilini, C., Gottardi, G., Govoni, L., Mentani, A., and Ubertini, F. (2015). Virtual testing of existing semi-rigid rockfall protection barriers. *Engineering Structures*, 85:83–94.

de Miranda, S., Gentilini, C., Gottardi, G., Govoni, L., and Ubertini, F. (2010). A simple model to simulate the full-scale behaviour of falling rock protection barriers. In *Proceedings of the 7th International Conference on Physical Modelling in Geotechnics-ICPMG*, volume 2, pages 103–108, Tokyo, Japan.

Eota (2013). ETAG 027 : Guideline for European Technical Approval of Falling Rock Protection Kits.

Escallòn, J. P., Wendeler, C., Chatzi, E., and Bartelt, P. (2014). Parameter identification of rockfall protection barrier components through an inverse formulation. *Engineering Structures*, 77:1–16.

Fang, K.-T., Li, R., and Sudjianto, A. (2005). *Design and Modeling for Computer Experiments*. Chapman and Hall/CRC, Boca Raton, FL.

Farhang-mehr, A. and Azarm, S. (2005). Bayesian meta-modeling of engineering design simulations: a sequential approach with adaptation to irregularities. *International Journal for Numerical Methods in Engineering*, 62:2104–2126.

Gentilini, C., Gottardi, G., Govoni, L., Mentani, A., and Ubertini, F. (2013). Design of falling rock protection barriers using numerical models. *Engineering Structures*, 50:96–106.

Gentilini, C., Govoni, L., de Miranda, S. d., Gottardi, G., and Ubertini, F. (2012). Three-dimensional numerical modelling of falling rock protection barriers. *Computers and Geotechnics*, Complete(44):58–72.

Gonzalez-Perez, C. and Henderson-Sellers, B. (2008). *Metamodelling for Software Engineering*. Wiley Publishing.

Jin, R., Chen, W., and Simpson, T. W. (2001). Comparative studies of metamodelling techniques under multiple modelling criteria. *Structural and Multidisciplinary Optimization*, 23(1):1–13.

Kausar, N., Samir, B. B., Abdullah, A., Ahmad, I., and Hussain, M. (2011). A Review of Classification Approaches Using Support Vector Machine in Intrusion Detection. In *Informatics Engineering and Information Science*, pages 24–34. Springer, Berlin, Heidelberg.

Kleijnen, J. P. C. (2009). Kriging metamodeling in simulation: A review. *European Journal of Operational Research*, 192(3):707–716.

Lambert, S. and Bourrier, F. (2013). Design of rockfall protection embankments: A review. *Engineering Geology*, 154:77–88.

Lambert, S., Bourrier, F., and Toe, D. (2013). Improving three-dimensional rockfall trajectory simulation codes for assessing the efficiency of protective embankments. *International journal of rock mechanics & mining sciences*, 60:26–36.

Lambert, S., Gotteland, P., and Nicot, F. (2009). Experimental study of the impact response of geocells as components of rockfall protection embankments. *Nat. Hazards Earth Syst. Sci.*, 9(2):459–467.

Ma, Y. and Ding, X. (2002). Face Detection Based on Cost-Sensitive Support Vector Machines. In *Pattern Recognition with Support Vector Machines*, pages 260–267. Springer, Berlin, Heidelberg. DOI: 10.1007/3-540-45665-1_20.

Maldonado, S. and LHuillier, G. (2013). SVM-Based Feature Selection and Classification for Email Filtering. In *Pattern Recognition - Applications and Methods*, Advances in Intelligent Systems and Computing, pages 135–148. Springer, Berlin, Heidelberg. DOI: 10.1007/978-3-642-36530-0_11.

Marelli, S. and Sudret, B. (2014). UQLab: A Framework for Uncertainty Quantification in Matlab. In *Vulnerability, Uncertainty, and Risk*, pages 2554–2563. American Society of Civil Engineers.

Martin, J. D. (2009). Computational Improvements to Estimating Kriging Metamodel Parameters. *Journal of Mechanical Design*, 131(8):084501–084501–7.

Mentani, A., Giacomini, A., Buzzi, O., Govoni, L., Gottardi, G., and Fityus, S. (2015). Numerical Modelling of a Low-Energy Rockfall Barrier: New Insight into the Bullet Effect. *Rock Mechanics and Rock Engineering*, 49(4):1247–1262.

Mentani, A., Govoni, L., Gottardi, G., Lambert, S., Bourrier, F., and Toe, D. (2016). A New Approach to Evaluate the Effectiveness of Rockfall Barriers.

Procedia Engineering, 158:398–403.

Mollon, G., Dias, D., and Soubra, A. (2011). Probabilistic Analysis of Pressurized Tunnels against Face Stability Using Collocation-Based Stochastic Response Surface Method. *Journal of Geotechnical and Geoenvironmental Engineering*, 137(4):385–397.

Mountrakis, G., Im, J., and Ogole, C. (2011). Support vector machines in remote sensing: A review. *ISPRS Journal of Photogrammetry and Remote Sensing*, 66(3):247–259.

Nicot, F., Cambou, B., and Mazzoleni, G. (2001). From a constitutive modelling of metallic rings to the design of rockfall restraining nets. *International Journal for Numerical and Analytical Methods in Geomechanics*, 25(1):49–70.

Sacks, J., Welch, W. J., Mitchell, T. J., and Wynn, H. P. (1989). Design and Analysis of Computer Experiments. *Statistical Science*, 4(4):409–423.

Simpson, T. W., Mauery, T. M., Korte, J. J., and Mistree, F. (2001). Kriging Models for Global Approximation in Simulation-Based Multidisciplinary Design Optimization. *AIAA Journal*, 39(12):2233–2241.

Sonnenburg, S., Rätsch, G., and Schölkopf, B. (2005). Large Scale Genomic Sequence SVM Classifiers. In *Proceedings of the 22Nd International Conference on Machine Learning*, ICML '05, pages 848–855, New York, NY, USA. ACM.

Sudret, B. (2008). Global sensitivity analysis using polynomial chaos expansions. *Reliability Engineering & System Safety*, 93(7):964–979.

Sudret, B. (2012). Meta-models for structural reliability and uncertainty quantification. *arXiv:1203.2062 [stat]*. arXiv: 1203.2062.

Thoeni, K., Lambert, C., Giacomini, A., and Sloan, S. W. (2013). Discrete modelling of hexagonal wire meshes with a stochastically distorted contact model. *Computers and Geotechnics*, 49:158–169.

Toe, D., Bourrier, F., Olmedo, I., Monnet, J.-M., and Berger, F. (2017). Analysis of the effect of trees on block propagation using a DEM model: implications for rockfall modelling. *Landslides*, pages 1–12.

Vapnik, V. (1995). *The Nature of Statistical Learning Theory*. Springer.

Volkwein, A. (2005). Numerical Simulation of Flexible Rockfall Protection Systems. *Computing in Civil Engineering*.

Zhang, Z., Xu, L., Flores, P., and Lankarani, H. M. (2014). A Kriging Model for Dynamics of Mechanical Systems With Revolute Joint Clearances. *Journal of Computational and Nonlinear Dynamics*, 9(3):031013–031013–13.